

Wobbling motion in the multi-bands crossing region

Makito Oi ^{a,d} ¹, Ahmad Ansari ^{a,b}, Takatoshi Horibata ^{c,d}
 Naoki Onishi ^{a,d}

^a*Institute of Physics, Graduate School of Arts and Sciences, University of Tokyo,
 Komaba, Meguro-ku, Tokyo 153-8902, Japan*

^b*Institute of Physics, Doordarshan Marg, Bhubaneswar 751 005, India*

^c*Department of Information System Engineering, Aomori University, Kobata,
 Aomori 030-0943, Japan*

^d*Cyclotron Laboratory, Institute of Physical and Chemical Research
 (RIKEN), Hirosawa 2-1, Wako-city, Saitama 351-0198, Japan*

Abstract

The backbending in the $A \simeq 180$ mass region is expected to be caused by multi-bands crossing between low- K (g- and s-bands) and high- K bands ($K^\pi = 8^+$ or 10^+). We analyze a mechanism of coupling of these bands in terms of a dynamical treatment for nuclear rotations, i.e., the wobbling motion. The wobbling states are produced through the generator coordinate method after angular momentum projection, in which the intrinsic states are constructed through the 2d-cranked HFB calculations.

Key words: wobbling motion, tilted rotation, band-crossing, signature, GCM, angular momentum projection

PACS number(s): 27.70.+q, 21.10.-k

A new interest in the “backbending” phenomenon has arisen through a series of experiments in 1990s’ [1–4] for nuclei in the $A \simeq 180$ region. It is expected that the backbending in this mass region is caused by the three-bands crossing, i.e., the ground (g-), super (s-) and “tilt” (t-) bands [4,5], unlike the backbending caused by the two-bands crossing of the g- and s-bands [6] in light rare-earth nuclei. The t-band was recently proposed as “tilted rotational band” [7]. In nuclei in the $A \simeq 180$ region, the Fermi level lies in states of high- Ω (Ω is a projection of single-particle angular momentum onto the symmetry axis of a nucleus). As a result, low- Ω states associated with the rotation-alignment are mostly occupied. Therefore, it is natural to expect a new type of excited bands

¹ e-mail address: mon@cns.s.u-tokyo.ac.jp

involving the high- Ω states. Hereafter we refer to the bands as high- K bands. Such bands as $K^\pi = 8^+$ (10^+) are actually observed in the vicinity of the yrast line ² in ^{180}W and ^{182}Os [1,2] (^{182}W and ^{184}Os [3,4]). It is characteristic that these bands have inter-band E2 transitions towards the yrast band having low- K configurations, namely these transitions violate the K -selection rule to a great extent ($\Delta K \simeq K$). Walker et al. considered that these transitions are related to a new type of the backbending mechanism involving tilting degrees of freedom in the rotation axis [1]. The nature of the high- K bands changes at lower and higher spin than that in the backbending region ($I_c \simeq 14\hbar$). At $I < I_c$, the bands form a regular $\Delta I=1$ sequence, while at $I > I_c$ the bands split into two $\Delta I=2$ sequences. After the splitting, the odd-spin sequence becomes energetically lower than the even-spin one, although the high- K bands begin with even spin ($I = 8\hbar$ or $10\hbar$). This type of splitting is conventionally called “signature inversion”. These features in the high- K bands suggest a certain strength of inter-band interaction between the low- and high- K bands.

There are, at least, two modes that couple states having intrinsic structures different in the K -quantum number. One is the wobbling motion that we present in this letter and the other is the triaxial deformation (i.e., sizeable γ deformation). In our recent calculations based on the two-dimensional cranked HFB (2d-CHFB) [8], the intrinsic states of $^{182,184}\text{Os}$ have (almost stable) prolate shape ($\gamma < 3^\circ$; $\beta \simeq 0.275$) in the backbending region ($I \simeq I_c$). Also, the calculations show that tilting and γ degrees of freedom are almost decoupled in the region, while the coupling is seen in the *very* high-spin region like $I \simeq 36\hbar$. In this letter, we focus on the wobbling motion decoupled from the γ -degree of freedom in $I \simeq I_c$.

The conventional cranking model, which is restricted to the rotation about the principal axis of the mass quadrupole deformation (PAR), can be extended to the rotation about an axis tilted away from the principal axis (TAR). PAR simulates low- K bands such as the g- or s-bands, while TAR describes high- K bands. In the present paper, both the PAR and TAR are calculated self-consistently through the 2d-CHFB method. We regard the wobbling motion as a dynamical mode to couple the low- and high- K states in a quantal and microscopic approach. We treat the motion in terms of the generator coordinate method after the angular momentum projection (*GCM after AMP*), in which tilt angle of the rotating axis is chosen to be the generator coordinate.

In our previous paper [11], we presented calculations based on the wobbling model (GCM based on 2d-CHFB wave functions) *without* angular momentum projection and encountered a difficulty in solving the Hill-Wheeler equation: a problem concerned with convergence in the eigenvalues with respect to the

² “yrast line” means a sequence of the lowest states in energy for given angular momentum.

“cut-off” dimension, which we will discuss below. We tried to improve the method through the constrained Hill-Wheeler equation, but could not obtain satisfactory results [12]. All the difficulties seem to come from the broken symmetries by the mean field approximation. (Angular momentum and numbers of nucleons are not conserved in deformed HFB states.) In many cases, the number constraints may be good enough to produce the reasonable cranked HFB states of stable nuclei [13,14]. We consider that, in a study of high-spin states, restoration of the rotational symmetry is more important than the gauge invariance, as the first attempt to circumvent the difficulties.

The 2d-CHFB states are wave packets of eigenstates in angular momentum (and number) and have broad width around the constrained value J [10,14]. Thus, the GCM states also include substantial components of undesirable angular momenta far from $I = J$. In order to eliminate them, we perform exact angular momentum projection (AMP) on 2d-CHFB states. Norm and energy overlap kernels are obtained through the formula [15]. But the well-known ambiguity of the phase by π inheres in the formula for the norm overlap kernels. We employ the analytic continuation method to determine the proper branches. [16].

The parameter set of the pairing+Q·Q model Hamiltonian employed here and details of the self-consistent 2d-CHFB method are found in Ref.[8]. In the 3d-cranking model, constraints on three components of angular momentum $J_k = \langle \Phi | \hat{J}_k | \Phi \rangle$ are specified by the tilting angle (θ, ϕ) and J through $J_1 = J \cos \theta \cos \phi$, $J_2 = J \cos \theta \sin \phi$ and $J_3 = J \sin \theta$. Here, a cranked HFB state is solved for ^{182}Os and denoted as $|\Phi(\theta\phi; J)\rangle$. The latitude (θ) and longitude (ϕ) angles are introduced so as to measure the deviation of the rotating axis from the x -axis (PAR).

Now, we set up a wobbling state, or GCM state ($|\Psi\rangle$), which is described as the superposition of projected 3d-cranked HFB states with different tilting angle:

$$|\Psi_M^I\rangle = \sum_{K=-I}^I \int_{-\theta_0}^{\theta_0} d\theta \int_{-\phi_0}^{\phi_0} d\phi f_K^I(\theta\phi) \hat{P}_{MK}^I |\Phi(\theta\phi; J)\rangle, \quad (1)$$

where \hat{P}_{MK}^I is the angular momentum projection operator [14]. The function $f_K^I(\theta, \phi)$ is called the generator wave function. The azimuthal angle ϕ_0 is taken to be zero in the present calculations and is omitted hereafter. As for θ_0 on the integration limit, we will explain later. J is fixed to be $14\hbar$, and we also see later some properties of the CHFB states with a constraint $J = 14\hbar$ briefly. The GCM state is obtained by the variational principle with respect to $f_K^I(\theta)$,

leading to the so-called Hill-Wheeler equation:

$$\sum_{K'} \int d\theta' \left(H_{KK'}^I(\theta, \theta') - E^I N_{KK'}^I(\theta, \theta') \right) f_{K'}^I(\theta') = 0. \quad (2)$$

The norm and energy overlap matrix-kernel $N_{KK'}^I(\theta, \theta')$ and $H_{KK'}^I(\theta, \theta')$ are respectively defined as follows,

$$\begin{pmatrix} N_{KK'}^I(\theta, \theta') \\ H_{KK'}^I(\theta, \theta') \end{pmatrix} = \begin{pmatrix} \langle \Phi(\theta) | \hat{P}_{KK'}^I | \Phi(\theta') \rangle \\ \langle \Phi(\theta) | \hat{H} \hat{P}_{KK'}^I | \Phi(\theta') \rangle \end{pmatrix}. \quad (3)$$

We solve Eq.(2) in two steps [11]: (1) Diagonalize the norm overlap matrix kernel like,

$$\sum_{K'} \int_{-\theta_0}^{\theta_0} d\theta' N_{KK'}^I(\theta, \theta') \chi_n^{IK'}(\theta') = \nu_n^I \chi_n^{IK}(\theta), \quad (4)$$

to obtain eigenvalues ν_n^I and eigenfunctions $\chi_n^{IK}(\theta)$, in which n is an index specifying ν_n^I in order of magnitude. The eigenvalues are never negative owing to properties of the norm overlap matrix-kernels; (2) Define energy matrices on the base of orthonormal set $|nIM\rangle = \sum_K \int_{-\theta_0}^{\theta_0} d\theta \chi_n^{IK}(\theta) / \sqrt{\nu_n^I \hat{P}_{MK}^I} | \Psi(\theta) \rangle$

$$\mathcal{H}_{nn'}^I = \sum_{KK'} \iint d\theta d\theta' \frac{\chi_n^{IK*}(\theta)}{\sqrt{\nu_n^I}} H_{KK'}^I(\theta, \theta') \frac{\chi_{n'}^{IK'}(\theta')}{\sqrt{\nu_{n'}^I}}. \quad (5)$$

Eventually, the Hill-Wheeler equation gets transformed into an eigenvalue equation: $\sum_{n'} \mathcal{H}_{nn'} g_{n'} = E^I g_n$. Integrations in Eq.(5) are achieved numerically by an approximation of discretization. In the present study, five angular points are chosen ($|\Phi(J, \theta)\rangle; \theta = 0^\circ, \pm 7^\circ$ and $\pm 20^\circ$) under a condition: $\langle \Phi(\theta_i) | \Phi(\theta_{i+1}) \rangle < 0.9$, up to $|\theta_{\max}| = 20^\circ$. There are two reasons why we take only angles up to 20° . The first reason comes from a physical argument: according to the energy curve for the CHFB states with $J = 14\hbar$ (See the curve for $J = 15\hbar$ in Fig.4(a) in Ref.[8]), the first valley around $\theta = 0^\circ$ has an edge at $\theta = 20^\circ$. Realization of the wobbling motion around PAR is thus achieved approximately by the superposition of the CHFB states corresponding to this first valley. Although we should attempt to examine a global wobbling motion from $\theta = -90^\circ$ to $\theta = +90^\circ$, the present framework is satisfactory to study the mechanism of mixing between high- and low- K states. The second reason comes from numerical difficulty to calculate the norm kernels at larger tilt angles which include quite high frequency modes. For a precise treatment of overlap kernels we need much finer meshes in the Euler angles, but this

requirement in numerical calculations cannot be feasible within an available computation time.

The net dimension of the Hill-Wheeler equation turns out to be $n_{\max} = \{5 \times (2I + 1)\}$ for a given angular momentum (I). Fig.1 shows the spectrum of each band (the yrast, yrare, and second yrare band³) as a function of n_{cut} . A “plateau” indicates that the solutions (i.e., energy eigenvalues) are almost independent of the cut-off dimension, n_{cut} . This result implies a great advantage of AMP in comparison with our previous GCM calculations. From the results, we truncate at $n_{\text{cut}} = 11$ for all states except the $I = 17$ yrare state, in which we truncate at $n = 10$. The odd- I states in the first yrare band form “slopes”, *except* narrow plateaus formed around $n_{\text{cut}} = 10$. The reason for the appearance of the “slopes” may come from mixing of the states with the different particle number, i.e., “contaminations in number”, for we have not carried out number projection in this work. Though the “contaminations” make our discussion dubious, the dual projection in number and angular momentum is nothing but a heavy calculation consuming a great deal of computer time. At present, we leave an examination on the effect of number projection as a future study.

Fig.2 shows the resultant energy spectrum in the band crossing region. The signature splitting and inversion take place in the $I \geq 15\hbar$ region. The phase of the staggering is properly reproduced comparing with the experiment: odd- I states are energetically lower than even- I states. However, the amount of the splitting is much larger than experimental values. Our result is roughly 500 keV while the experiment is about 100 keV. There are several reasons for this discrepancy. There may be some argument for a choice of the pairing-plus-quadrupole force, but a more important factor is a set of parameters for the effective force. The parameters should be adjusted for calculations of the *GCM after AMP* states, though this procedure is again difficult because of the limit of the present computation resources. Thus, we have to keep using the same parameters as in the HFB calculations. Other possibility for the discrepancy is that we take a fixed J value ($J = 14\hbar$) in the CHFB states. For example, in this study, the projected states with $I = 17\hbar$ are projected out from the CHFB state with $J = 14\hbar$. To make a better projected states, it can be better to project out from the CHFB states with $J = 17\hbar$.

It is satisfactory that the $\Delta I=1$ band sandwiched between the two $\Delta I=2$ bands is reproduced⁴ in Fig.2. We are tempted to say this band structure is produced via multi-bands crossing among g, s, and high- K bands. However, we should note that the higher $\Delta I=2$ band does not have a g-band character but a s-band one. This result can be explained as below: we have fixed the an-

³ “yrare band” means a sequence of the first excited states from the yrast states.

⁴ We pick up the lowest three levels out of 11 levels in order to draw the Fig.2.

angular momentum constraint on $J = 14\hbar$, and the gap energy for neutron in this range of angular momentum is substantially reduced due to the rotation-alignment (Refer to the result in Ref.[8]). Therefore, our generating states have a good amount of the rotation-aligned component, i.e. a strong character of the s-band. Consequently, the upper $\Delta I=2$ band is of the s-band character instead of the g-band.

Backbending is not well reproduced in the present calculations. We can suppose that this deficiency is also due to the lack of the g-band components in our calculations because the g-band can contribute to up- or back-bending through its crossing with the s-band. To make a complete analysis of the three-bands crossing in ^{182}Os , we need to use, at least, two different CHFB states: one with low J and the other with high J , and perform the *GCM after AMP* calculations around at each angular momentum. However, for a practical reason, the present paper is dedicated to an intensive study of the mixing of low- and high- K states through the wobbling motion, which corresponds to the band crossing of the s-band with the t-band. This situation can happen just after the g-s crossing. As for the g-t crossing, we will discuss later.

Let us learn the obtained K distributions of the wave functions in the context of the interaction between the lowest two bands. For this purpose, we calculate overlaps between the wobbling (GCM) state and each spin-projected intrinsic state (i.e., 2d-CHFB states): $\langle \Phi(J, \theta) | \hat{P}_{MK}^{I\dagger} | \Psi_M^I \rangle \equiv g_K^I(\theta)$ [14], evaluated by using the formula,

$$g_K^I(\theta) = \sum_{n=1}^{n_{\text{cut}}} \sqrt{\nu_n} g_n \chi_n^{IK}(\theta). \quad (6)$$

Fig.3 shows the quantity $|g_K^I(\theta)|^2$ with respect to K for each θ value. In our calculations, the $I = 14\hbar$ and $I = 16\hbar$ states correspond to the states before and after the crossing, respectively. In $I = 14\hbar$, the yrast state shows a typical feature of the s-band: the major component is $K = 0$ and some fluctuations around it, i.e., $\frac{|\Delta K|}{2} \simeq 1\hbar$ or $2\hbar$. This feature implies that a good amount of the rotation-aligned components are induced in the 2d-CHFB states at $J = 14\hbar$. In turn, the yrare state has two large peaks at $K = \pm 8\hbar$, and one small peak at $K = 0\hbar$. These features indicate a typical high- K band. Most of the high- K components are brought about by TAR states ($|\theta| = 20^\circ$). The existence of the $K = 0$ component implies the inter-band interaction with the yrast band, though the interaction is weak due to the large difference in energy [8]. In the crossing region, one can expect that the mixing is supposed to be stronger as the two bands come closer. In $I = 16\hbar$, we can find that both of the yrast and yrare states have three peaks at $\pm 8\hbar$ and $K = 0$, indicating that the bands are mixed with each other after the crossing. In particular, the yrare states have the three comparable peaks at low- and high- K components. In these perturbed states, the high- K components come mainly from TAR

states while the low- K components are brought by PAR states. Hence, these states are interpreted as the wobbling states, namely, dynamically rotating states coupling the low- K PAR and high- K TAR states. On the other hand, odd- I states in the high- K band are much *less perturbed* according to the calculations. This is because the odd- I members are energetically isolated and have no partners lying nearby to couple (PAR has only even- I states).

This fact draws an interpretation for the signature inversion in the t-bands: The inter-band interaction between the s- and t-bands pushes up (down) the even- I states in the t-band (s-band). (Note that the s-band is the yrast after the crossing with the g-band.) This downward shift of the yrast band may enhance backbending, though it is not clearly seen in the present calculation. The interaction between the g- and t-bands is quite weak because the g-band is approximately the pure $K = 0$ state with small admixture of high- K components. As a consequence, the backbending in the $A \simeq 180$ region occurs not only due to the rotation-alignment mechanism dominating in the rare-earth, but also due to the mechanism of the wobbling motion, i.e., the low- and high- K interaction. On the other hand, the odd- I states are unperturbed and serve as reference states for the interaction energy.

In summary, we have investigated a mechanism of backbending and the signature inversion in ^{182}Os , by means of *GCM after AMP*, on the 2d-cranked HFB states. With this method, we have qualitatively reproduced the main feature of the level structure showing the signature inversion in the high- K band lying very closely to the yrast band. We interpret this result from a point of view of an inter-band interaction between the low- K and high- K bands. We have shown that the perturbed states have characters of the wobbling motion, that is, dynamical mode coupling low- K PAR and high- K TAR states. In terms of this wobbling model, we have discussed an enhancement of the backbending in the $A \simeq 180$ region, in which the typical rotation-alignment is somewhat suppressed due to the location of the Fermi level. It is also shown that AMP brings about a great advantage in stabilization of eigenvalues in the Hill-Wheeler equation. At the same time, we realize that number projection turns out be important since it may eliminate a “slope” owing to the “number contamination”, as we expand the GCM states with the orthonormal basis.

We would like to thank Dr. N. Tajima for discussions and suggestions on this work. Most of the computations have been done using the Vector Parallel Processor, Fujitsu VPP500/28 at RIKEN which are also gratefully acknowledged.

References

[1] P.M. Walker et al., Phys. Lett. **B309** (1993) 14.

- [2] T.Kutsarova et al., Nucl. Phys. **A587** (1995) 111.
- [3] T.Shizuma et al, Nucl. Phys. **A593** (1995) 247.
- [4] T.Shizuma et al, Phys.Lett.**B442** (1998) 53.
- [5] P.M.Walker, Proc. Int. Conf. on the future of nuclear spectroscopy, Crete, (1993).
- [6] F.S. Stephens and R.S. Simon, Nucl. Phys. **A183** (1972) 257.
- [7] S.Frauendorf, Nucl. Phys. **A557** (1993) 259c.
- [8] A. Ansari, M. Oi, N. Onishi and T. Horibata, Nucl.Phys.**A654** (1999) 558.
- [9] T. Horibata and N. Onishi, Nucl. Phys. **A596** (1996) 251.
- [10] M.Oi, N.Onishi, N.Tajima and T.Horibata, Phys. Lett. **B418** (1998) 1.
- [11] T. Horibata, M. Oi and N. Onishi, Phys. Lett. **B355** (1995) 433.
- [12] T.Horibata, M. Oi, N.Onishi and A.Anvari, Nucl. Phys. **A646** (1999) 277; Nucl. Phys. **A651** (1999) 435 .
- [13] E.Wüst, A.Anvari, and U.Mosel, Nucl.Phys. **A435** (1985) 477.
- [14] P.Ring and P.Schuck, *Nuclear Many-body Problem* (Springer Verlalg, Berlin,1980) .
- [15] N.Onishi and S.Yoshida, Nucl. Phys. **80** (1966) 367.
- [16] K.Hara, K.Hayashi, and P.Ring, Nucl. Phys. **A385** (1982) 14.
- [17] A.Kerman and N.Onishi, Nucl.Phys. **A361** (1981) 179.
- [18] A.Bohr and B.Mottelson, *Nuclear Structure Vol.II* (Benjamin, Massachusetts, 1975).

Figure Captions

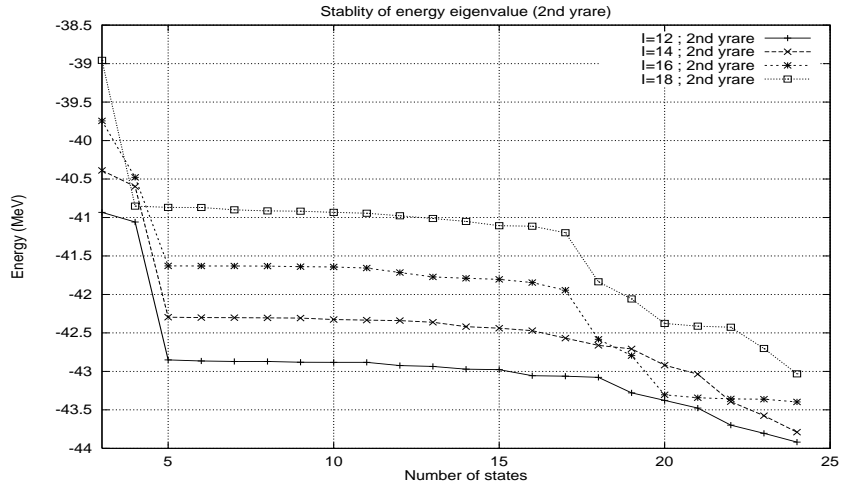
Fig.1 : A relation between the cut-off dimensions (n_{cut}) and the energy eigenvalues ($E^I(n_{\text{cut}})$) , in the Hill-Wheeler equation. The “plateaus” of the graphs imply the possibility of “safety cut-off” within the plateaus. In the present study, we choose $n_{\text{cut}} = 10$ for the first yrare $I = 17\hbar$ state and $n_{\text{cut}} = 11$ for the other states.

Fig.2 : Energy spectrum calculated through the *GCM after AMP*. The angular momentum constraint for the intrinsic state is fixed to be $J = 14\hbar$. From the analysis of the generator wave functions, the yrast and the second yrare bands ($\Delta I=2$ -bands) are of the low- K characters, while the first yrare band ($\Delta I=1$ -band) is of the high- K character. The signature inversion is seen at the region $I > 15\hbar$.

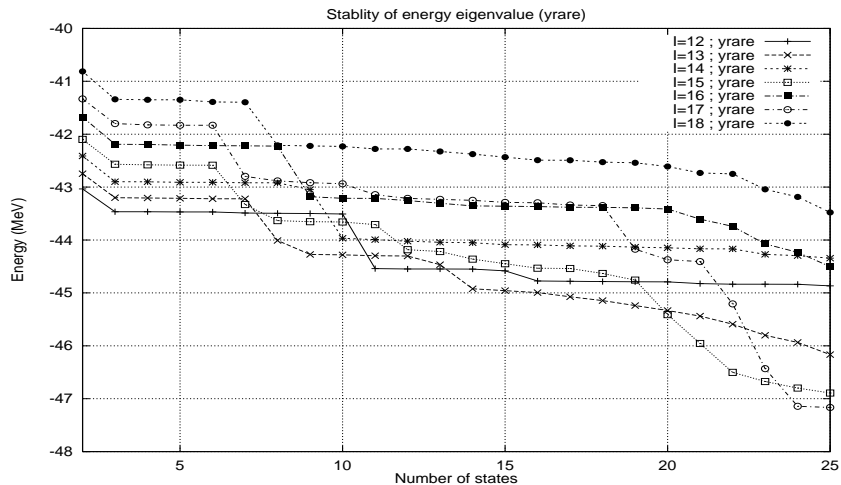
Fig.3 : Graphs for the overlaps between the GCM state and the spin-projected intrinsic state: $g_K^I(\theta) \equiv \langle \Psi(J, \theta) | \hat{P}_{MK}^{I\dagger} | \Psi_M^I \rangle$. (See texts.) The left panels are for the GCM states before the band crossing ($I = 14\hbar$), and the right panels are for the states after the crossing ($I = 16\hbar$). The lower and upper panels show the yrast and first yrare states, respectively. In each panel, the graphs are separately drawn for each tilt angle: $\theta = 0^\circ, \pm 7^\circ$, and $\pm 20^\circ$.

Stability of energy eigenvalues in the Hill-Wheeler equation

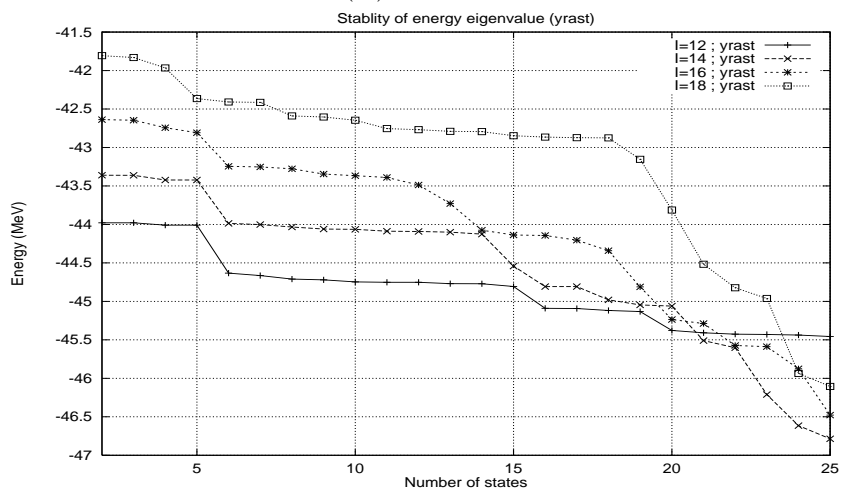
(i) Second yrare band



(ii) Yrare band



(iii) Yrast band



GCM Energy spectrum ($J=14$; $n=11$)

